https://cimav.repositorioinstitucional.mx/

Theoretical calculation of the maximum absorption wavelength for Cyanidin molecules with several methodologies

Nora-Aydee Sanchez-Bojorge, Luz-María Rodríguez-Valdez, Daniel Glossman-Mitnik, **Norma Flores-Holguín**

Abstract

Seven functionals, M06-L, M06, M06-2X, M06-HF, M11, PBE0 and B3LYP with two different basis set were used in the determination of the absorption spectrum in two chemical arrangements, Cyanidin (Cy) and Cyanidin-chloride (Cy-Cl). This second arrangement is studied trying to reproduce the ethanol/HCl environment of the experimental results. The main objective of this work is to find to find the influence of the electronic correlation and exchange in the absorption spectrum of Cy and Cy-Cl systems. The results of the calculated vertical excitation energies were affected by the Hartree–Fock exchange involved in the exchange–correlation functional. This can be clearly seen in the maximum absorption wavelength values found with the different methodologies applied, from which can be concluded that the best results are obtained with M06-L/6-31G(d) that predicts 547.93 nm followed by M06-L functional in combination with the 6-31G+(d,p) basis set with 544.3 nm. The experimental value is 547 nm. Also, a linear regression was performed comparing the calculated geometrical parameters with X-ray experimental data to define the best level of theory to reproduce with high precision the structural geometry, this is B3LYP/6-31+G(d,p).

https://cimav.repositorioinstitucional.mx/

1. Introduction

Flavonoids are constituted by a wide variety of molecules; anthocyanins represent the principal flavonoid group and are also considered natural dyes. They are responsible for the cyan shades ranging from salmon to dark blue in most flowers, fruits and leaves [1]. The basic structure of the anthocyanins is the anthocyanidins or aglycons, which consist of an aromatic ring (A) bonded to an heterocyclic ring (C) containing an oxygen atom, this ring is also bonded by a carbon–carbon bond to a third aromatic ring (B), Fig. 1(a). The distribution of the six most common anthocyanidins in fruits and vegetables is: Cyanidin 50%, Delphinidin 12%, Pelargonidin 12%, Peonidin 12%, Petunidin 7% and Malvidin 7% [2]. These have several advantages: availability, ease of synthesis or extraction, non-toxicicity, environmental safety and high biodegrability. Also, they have shown beneficial properties for human health, including antioxidant and antitumor activity [3], furthermore they have been broadly studied as photosensitizers for the dye sensitized solar cell (DSSC) [4] due to their visible-light harvest.

The charge-transfer process in DSSC involves several steps. The inciding photon is absorbed by the dye in its ground state; it is excited and injects an electron into the conduction band of the TiO_2 semiconductor; as a result the excited dye becomes oxidized. The injected electron travels through an external load and it is collected at the counter electrode, where it is then accepted by the redox couple present in the electrolyte. The cycle is completed with the reduction of the dye to its ground state [5]. An effective dye must have the energy level of its excited state inside the conduction band of the oxide semiconductor to carry out an effective

electron transfer. In addition, its redox potential should be high enough to regenerate due to electron donation from the electrolyte. Furthermore, it must absorb light within the solar spectrum from the UV to the near IR range [6]. Therefore, the study of the absorption spectrum and optical properties of dyes is essential in this type of devices.

In recent years, time-dependent density functional theory (TD-DFT), an important approach to the calculation of excitation energies, has been extensively used to study the structure and absorption spectra of sensitizing dyes for DSSCs [7]- [11]. It is an

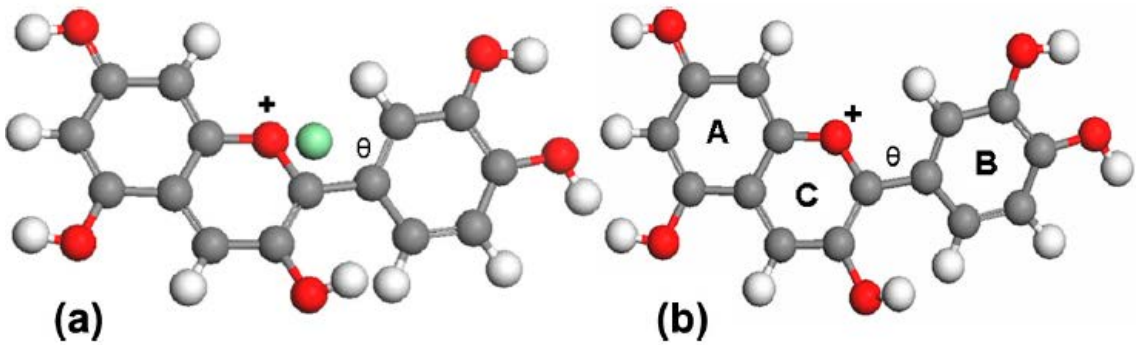

Fig. 1. Optimized geometry of Cyanidin-chloride (a) and Cyanidin (b).

important tool with low computational cost, based on the Kohn–Sham molecular orbital method, which gives a good molecular orbital description of the ground state electronic structure and the nature of the excitations. However, the TD-DFT transition energies are affected by the nature of the functional. The method achieves consistent values for the maximum absorption wavelength (λmax) and electronic transitions of dyes with different functionals; thus the functional proves crucial part to obtain high quality results.

https://cimav.repositorioinstitucional.mx/

Regarding functionals development, the local spin density functionals (LSDA) are considered the first generation of functionals, in which density functionals rely only on local densities, whereas the second generation of density functionals, is the generalized gradient approximation (GGA), in which functionals depend on the gradient of the electronic density as well as electronic density itself. The hybrid GGA functionals are determinated on the Hartree–Fock (HF) exchange and on the electronic density and its gradient. In the third generation of functionals, kinetic energy densities are included in the functional form; these functionals are called meta-GGAs. Hybrid meta-GGA functionals depend on the Hartree–Fock exchange, electronic density and its gradient as well as the kinetic energy density [12]. The functionals defined in the methodologies for this work were selected considering the notable progress in the development and validation of density functionals and considering the precision of a DFT calculation rests on upon the exchange–correlation (XC) quality.

In this work, we evaluate seven functionals combined with two Pople type basis set widely used to calculate organic dyes, in order to compare their performance predicting maximum wavelength of 2-(3,4 dihydroxyphenyl) chromenylium- 3,5,7-triol chloride (*Cyanidine chloride or Cy-Cl*) and 2-(3,4 dihydroxyphenyl) chromenylium- 3,5,7-triol (*Cyanidine or Cy*) dyes with experimental data, in an attempt to find the influence of the amount of electronic exchange of these functionals over this important property of common dyes used in DSSC. The Cy-Cl molecule calculation was performed in order to reproduce the ethanol/HCl environment. The methodology validation was accompanied with a linear regression,

https://cimav.repositorioinstitucional.mx/

without hydrogen atoms, of the calculated geometrical parameters compared with X-ray data [13]. Knowledge obtained from this study will aids in developing future calculations of the main principal properties of interest for this kind of molecules when used as photosensitizers.

2. Computational details

A PM3 semiempirical conformational analysis was performed for Cyanidin (Cy) and Cyanidin chloride (Cy-Cl) by using the Hyperchem 8.0 program [14] in order to find the most stable conformer considering the torsional angles. All the DFT computational calculations were carried out with the Gaussian 09W package [15]. Geometry optimization in solvent at the ground and excited states was performed. The force constants and vibrational frequencies calculations have also been carried out to check imaginary eigenvalues and to confirm for true minima structure.

The functionals used to carry out this study are: Perdew, Burkeand Ernzerhof, PBE0 [16] and Becke Three Parameter Lee, Yang, and Parr, B3LYP [17], both corresponding to the hybrid GGA functionals, which have shown good agreement with experimental values in organic dyes [18]; the M06 suite developed by Truhlar and coworkers at University of Minnesota, which consists of meta generalized gradient approximations (meta-GGAs) M06-L [19] and global-hybrid meta-GGAs, M06 and M06-2X [20], M06-HF [21] and M11 [22], functionals with different percentage of Hartree–Fock. All these functionals were combined with two Pople type basis sets: 6-31G(d) [23] and 6-31+G(d,p) [24].

The absorption spectra were calculated by solving the time-dependent density functional theory (TD-DFT) equations [25] ; [26]. The equations were solved for 20

https://cimav.repositorioinstitucional.mx/

excited states, where the computational studies were performed in presence Ethanol as solvent, using the IEFPCM (integral equation formalism PCM) method coupled to UAKS radii. In the PCM (Polarisable Continuum Model) scheme [27] ; [28], the solute molecule is placed in a shape-adapted cavity surrounded by the implicit solvent described as a continuum dielectric, which is characterized by its dielectric constant [29]. The IEF method originally developed by

Table 1
Correlation coefficients of bond distances for various methods used in geometry optimization of Cy and CyCl.

Compound	Functional	R^2
Cy	B3LYP/6-31G(d)	0.9285
	B3LYP/6-31+G(d,p)	0.9330
	M06/6-31G(d)	0.9147
	M06/6-31+G(d,p)	0.9176
	M06-2X/6-31G(d)	0.9191
	M06-2X/6-31+G(d,p)	0.9116
	M06HF/6-31G(d)	0.8913
	M06HF/6-31+G(d,p)	0.8813
	M06L/6-31G(d)	0.9139
	M06L/6-31+G(d,p)	0.9196
	M11/6-31G(d)	0.9227
	M11/6-31+G(d,p)	0.9146
	PBE0/6-31G(d)	0.9017
	PBE0/6-31+G(d,p)	0.9049
CyCl	B3LYP/6-31G(d)	0.9178
	B3LYP/6-31+G(d,p)	0.9202
	M06/6-31G(d)	0.8916
	M06/6-31+G(d,p)	0.8940
	M06-2X/6-31G(d)	0.9056
	M06-2X/6-31+G(d,p)	0.8880
	M06HF/6-31G(d)	0.8305
	M06HF/6-31+G(d,p)	0.8488
	M06L/6-31G(d)	0.9017
	M06L/6-31+G(d,p)	0.9061
	M11/6-31G(d)	0.8941
	M11/6-31+G(d,p)	0.8888
	PBE0/6-31G(d)	0.8940
	PBE0/6-31+G(d,p)	0.8944

https://cimav.repositorioinstitucional.mx/

Table 2
Exchange and correlation for methodology functionals.

Method	Exchange	X	Correlation
B3LYP	B88	20	LYP
PBE0	PBE	0	PBE
M06	M06	27	M06
M06-2X	M06-2X	54	M06-2X
M06-HF	M06-HF	100	M06-HF
M06-L	M06-L	0	M06-L
M11	M08	42.8	M08

Cances and Mennuci in 1997 [30]; [31] ; [32] introduces one function of permittivity dependent of the position, with this changes; the IEFPCM method presents better results than the original PCM method.

3. Results and discussion

3.1. Ground state calculations

The optimized structure and vibrational frequencies of Cyanidin (Cy) and Cyanidin-chloride (Cy-Cl) were calculated using seven different functionals and using the IEFPCM solvent model with ethanol as the solvent. The different levels of theory used for the ground state structure lead to geometrical parameters that have been compared with X-ray data [13] by performing linear regression analysis without hydrogen atoms; experimental results included bond distances exclusively. The largest R^2 is for B3LYP/6-31+G(d,p) for both molecules and second and third are for M06L/6-31+G(d,p) and M06L/6-31G(d,p) for Cy and for CyCl second and third are for B3LYP/6-31G(d) and M06L/6-31+G(d,p). The regression analysis results are shown in Table 1.

he structure is non-planar with the 2-phenyl ring twisted relative to the benzopyrylium rings in both systems, where the dihedral angle θ_1 (O13–C11–C20–

https://cimav.repositorioinstitucional.mx/

C21) fluctuates between 21 and 29 degrees, according to the methodology used and differs from the experimental values in an average of 12° which could be caused by the packing effect in the experimental crystals used. The orientation of the OH groups, even when they have free rotation, does not affect the molecule stability, remaining with the same orientation in all the different optimization achieved. The geometry optimization obtained with B3LYP/6-31+G(d,p) methodology describes with accuracy the ground state properties for Cy and CyCl. The obtained molecular structures are shown in Fig. 1.

3.2. Absorption calculations

The M06 suite functional was compared with the hybrid functionals B3LYP and PBE0 in order to analyze the effect of the Hartree–Fock exchange in the absorption spectrum. Seven of the considered functionals are hybrid and one of them is a local functional. Table 2 shows the exchange and correlation functionals included in each methodology used which were completed using the 6-31G (d) and 6-31+G (d,p) basis set.

The electronic absorption spectra were obtained using the time-dependent density functional theory (TD-DFT) and the functionals described above. The B3LYP/6-31+G(d,p) ground state equilibrium structure was used in these calculations. The IEFPCM solvent model was used with ethanol as solvent.

https://cimav.repositorioinstitucional.mx/

Table 3
Electronic absorption values for Cyanidin and Cyanidin-chloride obtained in ethanol as solvent by different methodologies.

Compound	Methodology	ΩA (eV)	Oscillator strength (f)	λmax (nm)	Electronic transition	
Cy	B3LYP/6-31G(d)	2.56	0.4104	484.61	H-0 → L+0(94%)	H-2-L+0(6%)
	B3LYP/6-31+G(d,p)	2.56	0.4311	483.75	H-0 → L+0(+93%)	H-2-L+0(+6%)
	M06/6-31G(d)	2.68	0.4864	463.03	H-0 → L+0(+93%)	
	M06/6-31+G(d,p)	2.66	0.469	466.44	H-0 → L+0(+91%)	H-1 → L+0(+6%)
	M06-2X/6-31G(d)	2.96	0.5562	419.24	H-0 → L+0(+86%)	H-1 → L+0(+12%)
	M06-2X/6-31+G(d,p)	2.93	0.5242	423.25	H-0 → L+0(+86%)	H-1 → L+0(12%)
	M06-HF/6-31G(d)	3.3	0.6543	376.11	H-0 → L+0(+82%)	H-1 → L+0(+13%)
	M06-HF/6-31+G(d,p)	3.28	0.6054	377.99	H-0 → L+0(+81%)	H-1 → L+0(13%)
	M06-L/6-31G(d)	2.26	0.2085	547.93	H-0 → L+0(80%)	H-1 → L+0(12%)
					H-2 → L+0(+8%)	
	M06-L/6-31+G(d,p)	2.28	0.2314	544.14	H-0 → L+0(+81%)	H-1 → L+0(10%)
					H-2 → L+0(8%)	
	M11/6-31G(d)	3.1	0.5874	400.49	H-0 → L+0(+81%)	H-1 → L+0(+16%)
	M11/6-31+G(d,p)	3.08	0.5461	402.16	H-0 → L+0(+81%)	H-1 → L+0(+15%)
	PBE0/6-31G(d)	2.69	0.4694	461.14	H-0 → L+0(+92%)	
	PBE0/6-31+G(d,p)	2.67	0.4527	463.66	H-0 → L+0(+90%)	H-1 → L+0(+6%)
CyCl	B3LYP/6-31G(d)	2.42	0.0282	512.90	H-1 → L+0(43%)	H-3 → L+0(36%)
					H-0 → L+0(17%)	
	B3LYP/6-31+G(d,p)	2.55	0.4172	485.28	H-0 → L+0(+94%)	H-5 → L+0(5%)
	M06/6-31G(d)	2.79	0.4568	444.77	H-3 → L+0(+91%)	
	M06/6-31+G(d,p)	2.64	0.3775	469.64	H-0 → L+0(+88%)	H-1 → L+0(+9%)
	M06-2X/6-31G(d)	2.99	0.4994	414.56	H-0 → L+0(+88%)	H-1 → L+0(+7%)
	M06-2X/6-31+G(d,p)	2.96	0.4871	419.06	H-0 → L+0(+88%)	H-1 → L+0(10%)
	M06-HF/6-31G(d)	3.34	0.6106	370.67	H-0 → L+0(+88%)	
	M06-HF/6-31+G(d,p)	3.31	0.5568	374.05	H-0 → L+0(+84%)	H-1 → L+0(+10%)
					H-0 → L+0(+59%)	H-1 → L+0(22%)
	M06-L/6-31G(d)	2.39	0.4253	519.69	H-2 → L+0(8%)	H-3 → L+0(6%)
					H-5 → L+0(5%)	
	M06-L/6-31+G(d,p)	2.44	0.3104	508.18	H-0 → L+0(+32%)	H-1 → L+0(9%)
	M11/6-31G(d)	3.14	0.5473	394.73	H-0 → L+0(+83%)	H-1 → L+0(+11%)
	M11/6-31+G(d,p)	3.11	0.5124	398.29	H-0 → L+0(+83%)	H-1 → L+0(+13%)
	PBE0/6-31G(d)	2.64	0.0945	469.82	H-1 → L+0(+53%)	H-0 → L+0(+27%)
					H-2 → L+0(12%)	H-3 → L+0(+8%)
	PBE0/6-31+G(d,p)	2.74	0.3956	451.84	H-3 → L+0(88%)	H-0 → L+0(+5%)
	λmax Experimental value 547 nm [34].					

The effect of the polarization and diffusion functions was analyzed and it has been observed that the use of the higher order polarizations from d to d,p and one diffusion function is added, the maximum absorption wavelength (λmax) changes only in 2 or 3 nm for the Cy molecule. For the CyCl molecule the change when the basis set is extended remains in 4 nm and the largest alteration is found around 30 nm and the B3LYP functional is used. The use of higher order polarizations and diffuse functions were explored by other authors in cyanine dyes and the change was not larger than 11 nm and the computational time was considerably increased [33]. For this reason we decided to test only the 6-31G(d) and 6-

https://cimav.repositorioinstitucional.mx/

31+G(d,p) basis set for the seven functionals defined for the TD-DFT calculations.

In Table 3, the TD-DFT results for Cy and Cy-Cl obtained with each functional and the two basis set mentioned above are summarized. It contains the experimental maximum absorption wavelength (λmax) [34] and the calculated one, the vertical absorption values (ΩA), the oscillator strength (*f*), and the contributing transitions. It can be seen in Table 3 that the change of the functional affects significantly the λmax for both molecules and that the results for the Cy molecule exhibit a better agreement than the Cy-Cl with the experimental maximum absorption wavelength (547 nm).

The analysis of the λmax calculated shows that the functionals with moderate HF exchange, M06 and PBE0 (with 27% and 25% respectively), underestimate the λmax by 84 nm for Cy molecule with both basis set and for CyCl 78 nm. Functionals with higher HF exchange such as M06-2X (54% HF exchange) and M06-HF (with 100% HF exchange) exhibit the major difference between the experimental and theoretical λmax value M06-2X undervalue 124 nm for Cy and 128 nm for CyCl molecules while the 100% HF exchange produces a considerable underestimation of 170 and 177 nm for Cy and CyCl molecules respectively. The functional M06-L with 6-31G(d) provides the best correlation with the experimental λmax.

For all methodologies, the main transition described in λmax corresponds to the frontier molecular orbitals HOMO (highest occupied molecular orbital) to LUMO (lowest unoccupied molecular orbital). The calculated vertical excitation energies show a dependency with the amount of Hartree–Fock exchange involved in the exchange–correlation functional, the larger the Hartree–Fock exchange, the larger

https://cimav.repositorioinstitucional.mx/

the vertical excitation with exception of M11with 42.8% exchange.

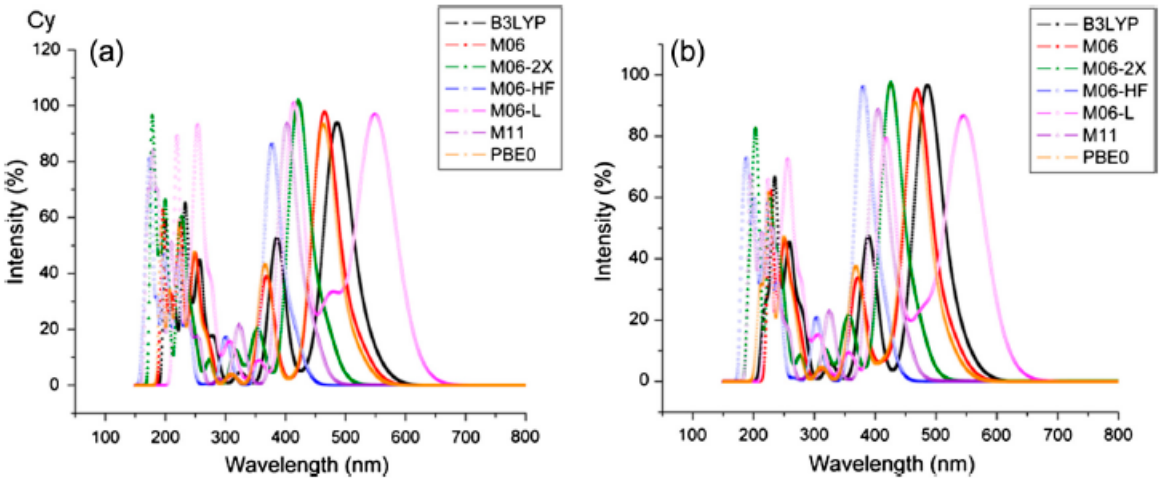

Fig. 2. UV/Vis spectra of Cyanidin obtained with different functionals in addition to (a) 6-31G(d) and (b) 6-31+G(d,p) basis set.

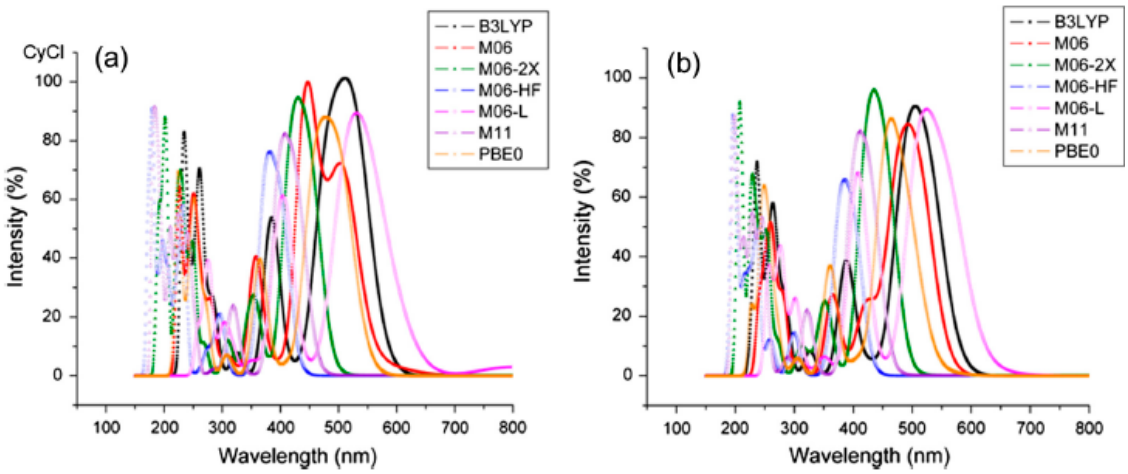

Fig. 3. UV/Vis spectra of Cyanidin Chloride (Cy-Cl) calculated with different functionals in addition to (a) 6-31G(d) and (b) 6-31 +G(d,p) basis set.

This can be attributed to the fact that vertical excitation energies are determined by the energy between the occupied and unoccupied molecular orbitals, which are affected by the Hartree–Fock exchange amount [35].

The UV/VIS spectra of cyaniding Cy calculated with different functional and 6-31G(d) and 6-31+G(d,p) basis set are shown in Fig. 2. As can be seen, the

https://cimav.repositorioinstitucional.mx/

functional B3LYP (with 20% HF exchange) reproduces with an hypsochromic shift of 63 nm with the experimental value while M06-L (0% HF exchange) repeat exactly the experimental maximum absorption wavelength.

The same theoretical behavior described for the Cy molecule was observed in the results with M06-L functional for the Cy-Cl system, which exhibits the best correlations with the experimental absorption wavelength of 547 nm with a theoretical value of 519 nm. The UV/VIS spectra calculated for Cy-Cl are shown in Fig. 3. In this particular molecule, the difference between the experimental and theoretical results was larger than for the Cy molecule.

The most accurate wavelength obtained with M06-L/6-31G(d) shows that this combination of functional and basis set is the best to reproduce the excited state properties, but B3LYP/6-31G(d) differs only by 35 nm. This functional was the best for predicting the ground state equilibrium structure and with this observation, we can define that the ground and excited states can be calculated with high precision with B3LYP.

However, taking into account that the aim of this study is to find a functional that provides the best approach to the experimental maximum absorption wavelength and considering the effect of the amount of the Hartree–Fock exchange in this property, the indication to carry out the calculation for this kind of molecules is for defining the minimal energy structure with B3LYP and the TD-DFT calculations using M-06L and a regular size basis set as 6-31G(d) without a computational time high demand.

https://cimav.repositorioinstitucional.mx/

4. Conclusions

In the current work, the absorption spectra for Cyanidin and Cyanidin-Chloride by TD-DFT based quantum-chemical methods were studied with seven different functionals, exhibiting several combinations of exchange and correlation and two Pople type basis set, 6-31G(d) and 6-31+G(d,p) for geometry optimization after a semiempirical conformational analysis and for the excited state calculation. The main objective was to find the influence of the electronic correlation and exchange in the absorption spectrum of Cy and Cy-Cl systems. The results showed that functionals with minor Hartree–Fock exchange amount exhibit a better correlation to the experimental value for the electronic absorption properties of the Cy molecule. The calculated vertical excitation energies were affected by the Hartree–Fock exchange involved in the exchange–correlation functional and after a careful inspection of different functionals, we recommend B3LYP functional to optimize the geometry and the M06-L as the optimum functional to find the maximum absorption wavelength for this kind of structures. The basis set effect is not significant to the equilibrium structure determination nor to the absorption wavelength definition.

Acknowledgments

This work was supported by Consejo Nacional de Ciencia y Tecnología (CONACYT) and Centro de Investigación en Materiales Avanzados, S.C. (CIMAV), and Universidad Autónoma de Chihuahua. NASB gratefully acknowledge a fellowship from CONACYT. N.F.H. and DGM are researchers of CIMAV and CONACYT and LMRV is a researcher for UACH and CONACYT.

https://cimav.repositorioinstitucional.mx/

References

[1] M.R. Narayan, Review: dye sensitized solar cells based on natural photosensitizers, Renew. Sust. Energy Rev. 16 (2012) 208–215.

[2] A. Castañeda-Ovando, M.L. Pacheco-Hernández, M.E. Páez-Hernández, J.A. Rodríguez, C.A. Galán-Vidal, Chemical studies of anthocyanins: a review, Food Chem. 113 (2009) 859–871.

[3] J.N. Woodford, A DFT investigation of anthocyanidins, Chem. Phys. Lett. 410 (2005) 182–187.

[4] Chiang-Yu Chien, Ban-Dar Hsu, Optimization of the dye-sensitized solar cell with anthocyanin as photosensitizer, Solar Energy 98 (2013) 203–2011.

[5] J. Simiyu, B.O. Aduda, J.M. Mwabora, Antocyanin-sensitized nanoporous TiO2 photoelectrochemical solar cells prepared by a sol–gel process, Prog. Colloid Polym. Sci. 125 (2004) 34–37.

[6] Jie Xu, Hui Zhang, Guijie Liang, Luoxin Wang, Xu Weilin, Wwigang Cui, Li Zengchang, DFT studies on the electronic structures of indoline dyes for dye-sensitized solar cells, J. Serb. Chem. Soc. 75 (2010) 259–269.

[7] T.R. Heera, L. Cindrella, Evaluation and visualisation of molecular orbitals of natural pigments by density functional theory for their application in photoelectrochemical devices, Mol. Simul. 36 (2010) 1–4.

[8] C. Qin, A.E. Clark, DFT characterization of the optical and redox properties of natural pigments relevant to dye-sensitized solar cells, Chem. Phys. Lett. 438 (2007) 26–30.

[9] Z. Liu, Theoretical studies of natural pigments relevant to dye-

https://cimav.repositorioinstitucional.mx/

sensitized solar cells, J. Mol. Struct.-Theochem. 862 (2008) 44–48.

[10] A.A. Freitas, K. Shimizu, L.G. Dias, F.H. Quina, J. Braz, A computational study of substituted flavylium salts and their quinonoidal conjugate-bases: S0 ? S1 electronic transition, absolute pKa and reduction potential calculations by DFT and semiempirical methods, J. Braz. Chem. Soc. 18 (2007) 1537–1546.

[11] Sheng Meng, Jun Ren, Efthimios Kaxiras, Natural dyes adsorbed on TiO2 nanowire for photovoltaic applications: enhanced light absorption and ultrafast electron injection, Nano Lett. 8 (2008) 3266–3272.

[12] Y. Zhao, D.G. Truhlar, Density functionals with broad applicability in chemistry, Acc. Chem. Res. 41 (2008) 157–167.

[13] Kathuhiko Ueno, Cyanidin bromide monohydrate (3,5,7,30,40-pentahydroxyflavylium bromide monohydrate), Acta Cryst. B33 (1977) 114–116.

[14] HyperChem(TM) Professional 7.51, Hypercube Inc., 1115 NW 4th Street, Gainesville, Florida 32601, USA.

[15] M.J. Frisch, Gaussian 09, Revision A.1 Gaussian Inc., Wallingford CT, 2009

[16] C. Adamo, V. Barone, Toward reliable density functional methods without adjustable parameters: the PBE0 model, J. Chem. Phys. 110 (1999) 6158–6169.

[17] A.D. Becke, Density-functional thermochemistry. III. The role of exact exchange, J. Chem. Phys. 98 (1993) 5648–5652.

https://cimav.repositorioinstitucional.mx/

[18] P. Ekanayake, M.R.R. Kooh, N.T.R.N. Kumara, A. Lim, M.I. Petra, N.Y. Voo, C.M. Lim, Combined experimental and DFT–TDDFT study of photo-active constituents of Canarium odontophyllum for DSSC application, Chem. Phys. Lett. 585 (2013) 121–127, http://dx.doi.org/10.1016/j.cplett.2013.08.094.

[19] Y. Zhao, D.G. Truhlar, A new local density functional for main-group thermochemistry, transition metal bonding, thermochemical kinetics, and noncovalent interactions, J. Chem. Phys. 125 (2006) 194101, http://dx.doi.org/ 10.1063/1.2370993.

[20] Y. Zhao, D.G. Truhlar, The M06 suite of density functionals for main group thermochemistry, thermochemical kinetics, noncovalent interactions, excited states, and transition elements: two new functionals and systematic testing of four M06-class functionals and 12 other functionals, Theor. Chem. Acc. 120 (2008) 215–241.

[21] Y. Zhao, D.G. Truhlar, Density functional for spectroscopy: no long-range self-interaction error, good performance for Rydberg and charge-transfer states, and better performance on average than b3lyp for ground states, J. Phys. Chem. A 110 (2006) 13126–13130, http://dx.doi.org/10.1021/jp066479k.

[22] R. Peverati, D.G. Truhlar, Improving the accuracy of hybrid meta-GGA density functionals by range separation, J. Phys. Chem. Lett. 2 (2011) 2810–2817. doi.org/10.1021/jz201170d |.

[23] G.A. Petersson, M.A. Al-Laham, A complete basis set model chemistry. II. Open-shell systems and the total energies of the first-row atoms, J. Chem. Phys. 94 (1991) 6081–6090.

https://cimav.repositorioinstitucional.mx/

[24] R. Ditchfield, W.J. Hehre, J.A. Pople, Self-consistent molecular orbital methods.

IX. An extended gaussian-type basis for molecular orbital studies of organic molecules, J. Chem. Phys. 54 (1971) 724.

[25] L. Bartolloti, Time-dependent Kohn–Sham density-functional theory, J. Phys. Rev. A 26 (1982) 2243–2244.

[26] E. Runge, E.K.U. Gross, Density-functional theory for time-dependent systems, Phys. Rev. Lett. 52 (1984) 997–1000.

[27] C. Amovilli, V. Barone, R. Cammi, E. Cancés, M. Cossi, B. Mennucci, C.S. Pomelli,

J. Tomasi, Recent advances in the description of solvent effects with the polarizable continuum model, Adv. Quantum Chem. 32 (1998) 27–261.

[28] J. Tomasi, B. Mennucci, R. Cammi, Quantum mechanical continuum solvation models, Chem. Rev. 105 (2005) 2999–3093.

[29] E.H. Anouar, J. Gierschner, J.L. Droux, P. Trouillas, UV/Visible spectra of natural polyphenols: a time-dependent density functional theory study, Food Chem. 131 (2012) 79–89.

[30] E. Cancés, B. Mennucci, J. Tomasi, A new integral equation formalism for the polarizable continuum model: theoretical background and applications to isotropic and anisotropic dielectrics, J. Chem. Phys. 107 (1997) 3032–3041.

[31] B. Mennucci, E. Cancés, J. Tomasi, Evaluation of solvent effects in isotropic and anisotropic dielectrics and in ionic solutions with a unified integral equation method: theoretical bases, computational implementation, and numerical

https://cimav.repositorioinstitucional.mx/

applications, J. Phys. Chem. B 101 (1997) 10506–10517.

[32] E. Cancés, B. Mennucci, New applications of integral equations methods for solvation continuuum models: ionic solutions and liquid crystals, J. Math. Chem. 23 (1998) 309–326.

[33] Sıla Karaca, Nuran Elmac, A computational study on the excited state properties of a cationic cyanine dye: TTBC, Comput. Theor. Chem. 964 (2011) 160–168.

[34] P. Ribereau-Gayon, Recherches sur les anthocyannes des vegetaux. Application au genre Vitis, Dissertation, University of Bordeaux, Paris, 1959.

[35] S. Uck Lee, Influence of exchange–correlation functional in the calculations of vertical excitation energies of halogenated copper phtalocyanines using time-dependent density functional theory (TD-DFT), Korean Chem. Soc. 34 (2013) 2276–2280.